The EMBO Journal vol.15 no.3 pp.498–509, 1996

Expression of V642 APP mutant causes cellular apoptosis as Alzheimer trait-linked phenotype

Tomoki Yamatsuji[1], Takashi Okamoto[2], Shizu Takeda[3], Yoshitake Murayama[4], Noriaki Tanaka[5] and Ikuo Nishimoto[6]

Cardiovascular Research Center, Massachusetts General Hospital, Department of Medicine, Harvard Medical School, Charlestown, MA 02129, USA, [4]Fourth Department of Medicine, University of Tokyo School of Medicine, Mejirodai, Bunkyo-ku, Tokyo 112 and [5]First Department of Surgery, Okayama University School of Medicine, Shikata-cho, Okayama, Okayama 700, Japan

[1]Present address: First Department of Surgery, Okayama University School of Medicine, Shikata-cho, Okayama, Okayama 700, Japan
[2]Present address: Shriners Hospitals for Crippled Children, Massachusetts General Hospital, Department of Anesthesia, Harvard Medical School, Boston, MA 02114, USA
[3]Present address: Laboratory of Molecular and Cellular Neuroscience, The Rockefeller University, 1230 York Avenue, New York, NY 10021, USA

[6]Corresponding author

T.Yamatsuji and T.Okamoto contributed equally to this work

APP is a transmembrane precursor of β-amyloid. In dominantly inherited familial Alzheimer's disease (FAD), point mutations V642I, V642F and V642G have been discovered in APP_{695}. Here we show that expression of these mutants (FAD-APPs) causes a clone of COS cells to undergo apoptosis associated with DNA fragmentation. Apoptosis by the three FAD-APPs was the highest among all possible V642 mutants; normal APP_{695} had no effect on apoptosis, suggesting that apoptosis by APP mutants in this system is phenotypically linked to the FAD trait. FAD-APP-induced apoptosis was sensitive to *bcl-2* and most probably mediated by heteromeric G proteins. This study presents a model system allowing analysis of the mechanism for FAD-APP-induced cytotoxicity.

Keywords: amyloid precursor protein/apoptosis/*bcl-2*/familial Alzheimer's disease/G proteins

Introduction

Alzheimer's disease (AD) is the most prevalent neurodegenerative disease, characterized by the presence of senile plaques, neurofibrillary tangles and extensive neuronal loss. Senile plaques are extracellular deposits whose major constituent is Aβ amyloid, the precursor of which, APP (Kang *et al.*, 1987), is located in cellular membrane systems including the cell surface. In AD, Aβ is cleaved off from APP and is deposited extracellularly. Alternative splicing of a single gene results in at least 10 isoforms of APP (Sandbrink *et al.*, 1994). APP_{695}, consisting of 695 residues, is expressed preferentially in neuronal tissues. In early-onset familial AD (FAD), missense mutations V642I/F/G have been identified in the transmembrane domain in APP_{695} (Goate *et al.*, 1991; Hardy, 1992). These mutations (APP_{V642X} is referred to as X-APP) co-segregate with AD phenotype (Karlinsky *et al.*, 1992) and account for most, if not all, of the evidence showing a linkage of AD to chromosome 21 (Hardy, 1992). Recently, Games *et al.* (1995) have reported that overexpression of Phe-APP mimics the neuropathology of AD in transgenic mice.

Nonetheless, little has been known about either the molecular function of APP_{695} or its abnormality shared by three FAD-APPs. Only secretion of Aβ1-42 has been reported to be a common target of Ile-APP and Phe-APP (Suzuki *et al.*, 1994). APP consists of a single transmembrane structure with a glycosylated extracellular domain and a short cytoplasmic domain which is well conserved in evolution. In addition, APP is involved in signaling of cell adhesion (Ueda *et al.*, 1989; Mönning *et al.*, 1992), neurite outgrowth (Milward *et al.*, 1992; Mattson *et al.*, 1993; Small *et al.*, 1994) and synaptic contact (Schubert *et al.*, 1991). While these functions have been shown with secreted APP, intact APP_{695} *per se* may serve as a cell surface receptor. Recently, APP gene knockout (Müller *et al.*, 1994; Zheng *et al.*, 1995) has suggested the essential role of APP in neuronal development and function. We have defined the receptor mimetic function in APP_{695} by multiple approaches, and have suggested that APP_{695} is a functional G_o-linked receptor (Nishimoto *et al.*, 1993; Okamoto *et al.*, 1995). This concept is in excellent agreement with the reports showing that G_o mediates signals for neuronal adhesion, contact and neurite outgrowth (Schuch *et al.*, 1989; Doherty *et al.*, 1991; Strittmatter *et al.*, 1994), all similar to the signals mediated by APP. As the dominant inheritance of this type of FAD suggests that the function of APP is dominantly abnormal in FAD-APPs, we theorized that FAD-APPs carry constitutively active G_o-linked receptor function and that cellular abnormality due to FAD-APP could be detected by transfecting the cognate cDNA into intact cells. Here, using a mammalian expression system we have examined whether apoptosis is an abnormal outcome executed by FAD-APP. The results show that apoptosis is a novel phenotype commonly induced by the three FAD-APPs in a manner linked to the FAD mutations. We also find that apoptosis by FAD-APP is antagonized by *bcl-2* and is mediated by a specific intracellular pathway involving heteromeric G proteins.

Results

We transiently transfected APP_{695} and FAD-APP cDNAs into COS-NK1 cells by the lipofection method. The constructs were expressed similarly and to comparable extents from 12–48 h after transfection, as assessed with immunoblotting (not shown) and immunohistochemistry (Figure 1). After transfection of FAD-APP, we examined the evidence for apoptosis in cells expressing FAD-APP.

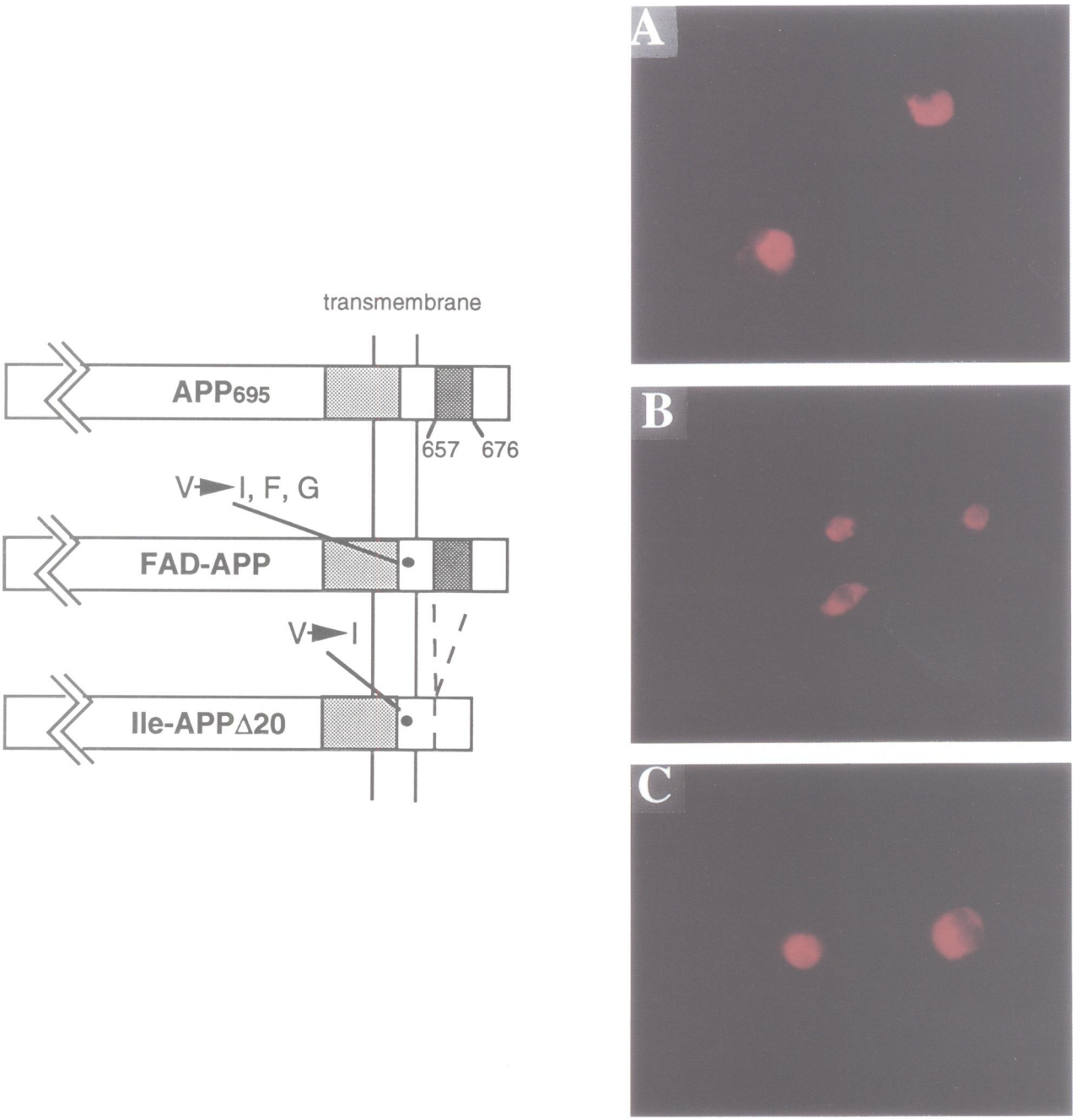

Fig. 1. Constructs of APP mutants and their expression in COS-NK1 cells. Left: APP_{695}, FAD-APPs (V642I, V642F, V642G) and Ile-APPΔ20 are illustrated. Right: immunohistochemical staining of Ile-APP (**A**), APP_{695} (**B**) and Ile-APPΔ20 (**C**) by anti-APP antibody after transfection of the cognate cDNAs. At 48 h after transfection of these APP cDNAs, the sample was fixed and stained with 22C11. Using this procedure, the cells expressing transfected FAD-APP were stained red and identified using fluoromicroscopy.

We first investigated DNA fragmentation, because it is a useful marker of apoptosis. After transfection, we assessed DNA fragmentation with the ELISA assay with two antibodies directed against histone and DNA. This immunoassay—which sensitively and selectively detects nucleosomally fragmented DNA—revealed that transfection of three FAD-APP cDNAs into COS-NK1 cells in each case augmented the production of oligonucleosomally fragmented DNA by 3- to 4-fold over that observed by mock-transfection or that observed in the cells not exposed to transfection (Figure 2A). These fragmentation levels were comparable with that caused by high concentrations of staurosporine, which induce apoptosis in many types of cells (Jacobson *et al.*, 1993). In contrast, transfection of APP_{695} cDNA did not significantly produce oligonucleosomally fragmented DNA as compared with LacZ transfection, despite a level of expression comparable with those of FAD-APPs and the fact that only one residue is different between FAD-APPs and APP_{695}. Thus, DNA fragmentation by FAD-APPs must not be an artifact of transfection. Although this assay does not exclusively detect apoptosis, it is clear that remarkable fragmentation of DNA is induced by expression of three FAD-APPs, but not of normal APP_{695}.

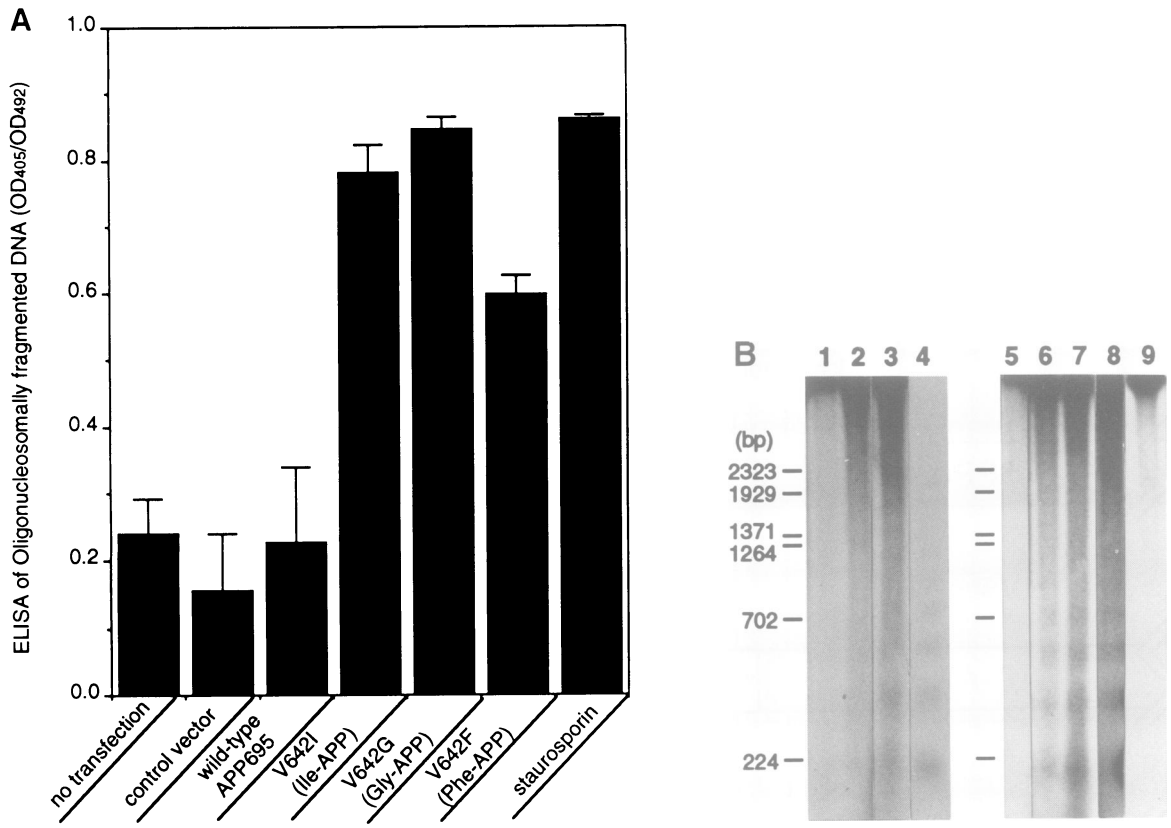

FAD-APP-induced DNA fragmentation is associated with the formation of a nucleosomal-size ladder of DNA. We radioactively end-labeled the preparations of DNA extracted from transfected COS-NK1 cells with Klenow polymerase. Typical chromatin fragmentation was observed in DNA extracted from COS-NK1 cells transfected with FAD-APP (Figure 2B). Transfection of FAD-APP cDNA (Figure 2B, lanes 3, 6, 7 and 8), but not of APP_{695} cDNA (Figure 2B, lane 2) or the negative control *lacZ* (Figure 2B, lanes 1 and 5), yielded nucleosome-length fragmentation of DNA in agarose gels as early as 12 h post-transfection, which was also observed in stronger intensities at 24 h post-transfection. The same condition without plasmids did not yield any ladder (Figure 2B, lane 9). The 180 bp fragmentation of DNA induced by FAD-APP transfection was similar to that observed in IL-3-deprived hematopoietic cells (Figure 2B, lane 4).

We also tested TdT-mediated dUTP nick end-labeling (TUNEL), which specifically stains the 3′ OH end of nucleosomally fragmented DNA with exogenous TdT and digoxigenin–dUTP and visualizes nucleosomal DNA fragmentation *in situ* (Gavrieli *et al.*, 1992). The nucleosomally fragmented DNA was finally visualized by anti-digoxigenin antibody conjugated with ALP. With this method, we detected nucleosomal DNA fragmentation *in situ* in COS-NK1 cells transfected with FAD-APP cDNA. Transfection of Ile-APP cDNA resulted in significantly increased staining of fragmented DNA (Figure 2C, center panel). In contrast, transfection of APP_{695} cDNA (Figure 2C, upper panel) or a vector (not shown) caused virtually no DNA fragmentation, suggesting that FAD-APP-induced TUNEL staining is not an artifact. Also, similar expression of Ile-APPΔ20 (Figure 1), an Ile-APP mutant lacking cytoplasmic 20 residues, caused no DNA fragmentation (Figure 2C, lower panel), again supporting the notion that a specific mechanism underlies this novel action of FAD-APP. Thus, it is shown here again that FAD-APP expression specifically causes COS-NK1 cells to undergo nucleosomal DNA fragmentation.

To examine whether apoptosis occurred in the same cell that expressed FAD-APP, we doubly stained FAD-APP and nuclei in COS-NK1 cells transfected with FAD-APP cDNA. Nuclear fragmentation, compaction and condensation are established definitions for apoptosis (Kerr and Harmon, 1991). We quantitated the percentage of the FAD-APP-positive cells (transfectant-induced incidence) and the percentage of the FAD-APP-negative cells (background incidence) undergoing apoptotic nuclear change. By comparing the background incidence with the transfectant-induced incidence, one can establish whether the expression of FAD-APP directly affects apoptosis. With this assay, we again observed 6- to 7-fold increases in the incidence of apoptosis by each FAD-APP, and no increase by APP_{695} as compared with that by LacZ (Figure 2D). Furthermore, 72 h after transfection, cytoplasmic condensation was observed in all FAD-APP-expressing cells (data not shown), and then they detached from the plates. Thus, FAD-APPs evoke typical apoptosis in the cell expressing these mutants.

Bcl-2 is a well-established inhibitor of apoptosis, and sensitivity to *bcl-2* is accepted as a major criterion for apoptosis. We thus examined whether Ile-APP-induced DNA fragmentation is sensitive to *bcl-2* in both transient and stable expression systems. When *bcl-2* cDNA was co-transfected into COS-NK1 cells, the incidence of apoptosis induced by Ile-APP expression was significantly reduced

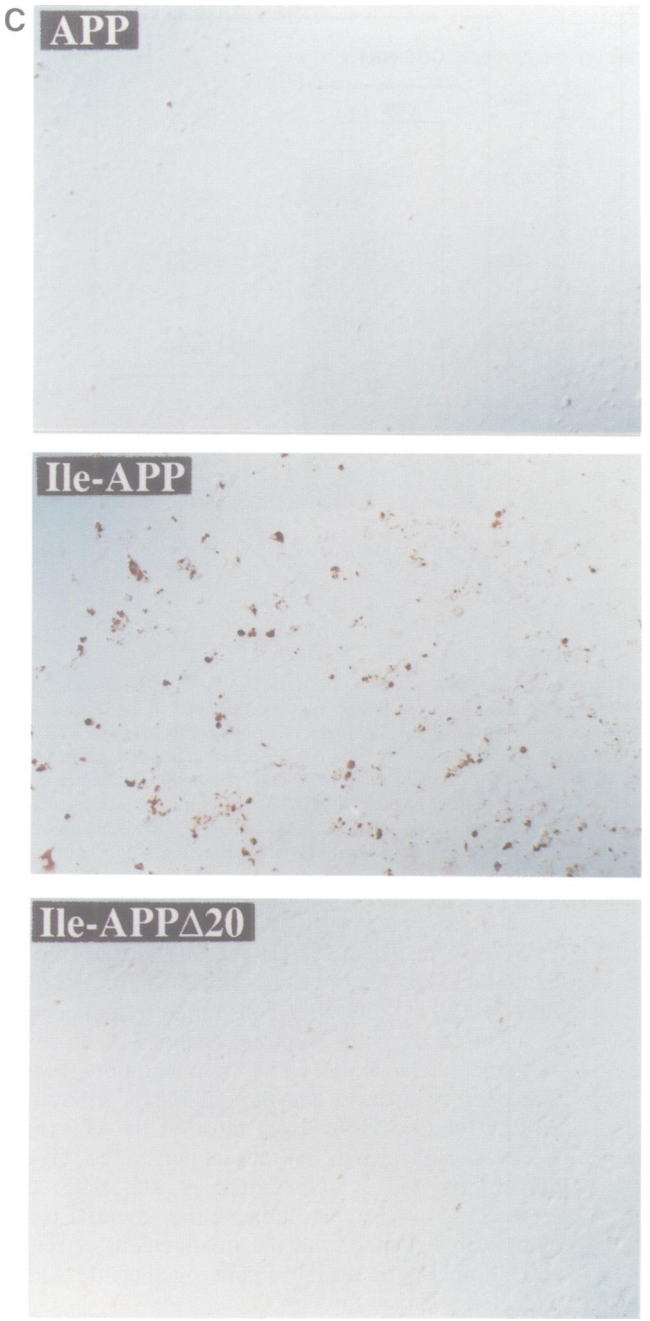

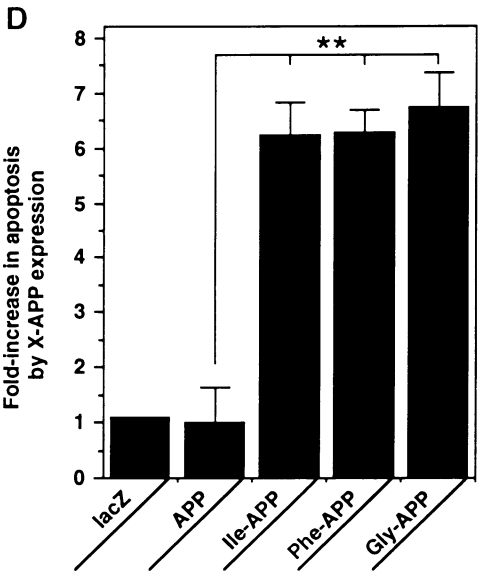

Fig. 2. FAD-APPs induce apoptosis in COS-NK1 cells. (**A**) By ELISA, fragmented DNA was measured at 48 h after transfecting COS-NK1 cells in a 24-well plate with a control vector, APP_{695} cDNA, or each FAD-APP cDNA. Three independent sets of transfection were done. Data indicate means (± SE) of histone-associated fragmented DNA (OD_{405}/OD_{492}) in the homogenate from an entire well. COS-NK1 cells were also treated with 1 μM staurosporine for 1 h in serum-free culture. (**B**) Cell death is accompanied by nucleosome laddering. COS-NK1 cells were transfected with *LacZ* (lanes 1 and 5), APP_{695} cDNA (lane 2), Ile-APP cDNA (lane 6), Phe-APP cDNA (lanes 3 and 7) and Gly-APP cDNA (lane 8). Cells were collected from a plate at 12 h (left panel) or 24 h (right panel) after transfection. DNA was isolated, radiolabeled by Klenow polymerase and fractionated on a 1.8% agarose gel. Lane 4, IL-3-deprived 32D hematopoietic cells (24-h deprivation); lane 9, COS-NK1 cells exposed to the transfection procedure for 24 h in the absence of plasmids. (**C**) TUNEL of transfected cells. COS-NK1 cells transfected with APP_{695} cDNA, Ile-APP cDNA or Ile-APPΔ20 cDNA and fixed at 48 h after transfection. The 3′ OH end of nucleosomally fragmented DNA was stained brown by TdT and labeled dUTP. The results in (B) and (C) are representative of three independent experiments, each of which yielded similar results. (**D**) Apoptosis occurs in the same cells that express FAD-APP. Cells were transfected with APP_{695} or each FAD-APP cDNA. At 48 h after transfection, the cells expressing transfected APP molecules were stained red with anti-APP antibody 22C11 and the nuclei of all cells were stained green with acridine orange. Red cells were counted throughout the well (= *a*) and the number of red cells having an apoptotic nucleus (= *b*). The incidence of apoptosis by FAD-APP was *b*/*a*. In each transfection, background incidence (*c*) of apoptosis was estimated by counting the frequency of APP-non-expressing cells that have apoptotic nuclei in the same sample. The subtraction (*b*/*a*)–*c*, represents the specific apoptosis induced by the expression of FAD-APP. The ratios of FAD-APP-induced specific apoptosis versus APP-induced are indicated. The specific apoptosis by APP_{695} was 14.4%. The background incidence of apoptosis was constantly ~20%, which represents transfection-induced non-specific cell damage and/or non-specific nuclear deformity, as TUNEL indicates that the death rate of FAD-APP-transfected cells in the background was negligible under the same condition. 0.5 μg *lacZ* gene was also transfected and visualized by XGal staining. Data indicate means (± SE) of three independent sets of transfection. In these experiments, the total numbers of APP- or FAD-APP-expressing cells were 615, 447, 594 and 228 for APP_{695}, Ile-APP, Phe-APP and Gly-APP, respectively. The LacZ data were from 798 LacZ-expressing cells. $^{**}P < 0.01$ by Student's *t* test

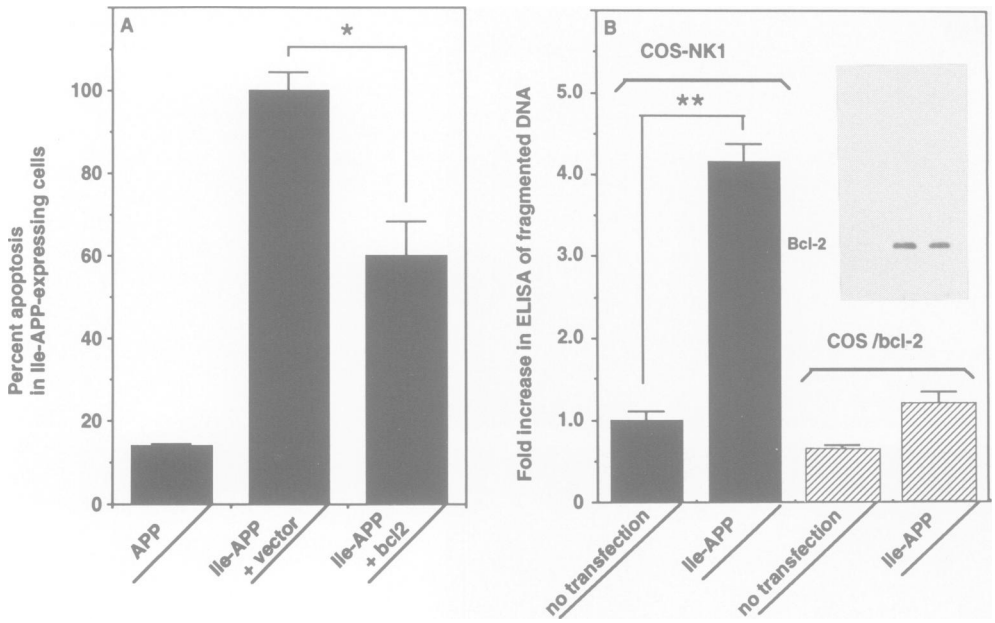

Fig. 3. Bcl-2 sensitivity of apoptosis by FAD-APP. (**A**) Transient transfection of *bcl-2* cDNA. At 48 h after transfecting COS-NK1 cells with 0.5 μg Ile-APP cDNA with 0.5 μg *bcl-2* cDNA or vector, apoptosis was assessed with apoptotic nuclear morphology as described in the legend of Figure 2D. The specific incidence of apoptosis [(*b*/*a*)–*c* in Figure 2D] is indicated as a percentage of Ile-APP-induced apoptosis, which was 42.7%. As a control, 0.5 μg APP cDNA was transfected. In co-transfection of *bcl-2* cDNA or vector, the levels of Ile-APP expression per cell did not differ. Data are means (± SE) of three independent sets of transfection. $*P < 0.05$. (**B**) The experiment using COS/*bcl-2* cells that stably overexpress Bcl-2. COS/*bcl-2* cells (right) or parental COS-NK1 cells (left) were transfected with or without 0.5 μg Ile-APP cDNA. At 48 h after transfection, oligonucleosomally fragmented DNA from a well was measured by ELISA. In this figure, 100% indicates 0.125 as OD_{405}/OD_{492}, which represents the DNA fragmentation of non-transfected COS-NK1 cells. Data are means (± SE) of three independent sets of transfection. $**P < 0.01$. Inset: Immunoblot analysis of Bcl-2 in COS-NK1 cells (left), COS/*bcl-2* cells (middle), COS/*bcl-2* cells transiently transfected with Ile-APP cDNA (right). The cell homogenate (100 μg) from each cell line was subjected to immunoblot analysis using anti-Bcl-2 antibody (DAKO, 1/500).

(Figure 3A). We also tested the sensitivity to *bcl-2* in COS-NK1 cells stably overexpressing Bcl-2 (COS/*bcl-2* cells) (Figure 3B, inset). The expression level of Bcl-2 was not affected by Ile-APP transfection. As shown, the efficacy of Ile-APP in causing DNA fragmentation was drastically impaired in COS/*bcl-2* cells, as compared with that in parental cells. The expression levels of transfected Ile-APP were similar in COS-NK1 and COS/*bcl-2* cells (data not shown). Thus, FAD-APP-induced DNA fragmentation is sensitive to *bcl-2*, providing evidence that FAD-APP causes COS-NK1 cells to undergo *bcl-2*-sensitive apoptosis.

The occurrence of death in the same cells that express FAD-APP indicated that FAD-APP turned on the intracellular pathways *in situ* that cause apoptosis. As G_o functions as a signal transducer of APP_{695} (Nishimoto *et al.*, 1993; Okamoto *et al.*, 1995), we next examined the involvement of this and other G proteins in apoptosis by FAD-APP. When these cells were treated with pertussis toxin (PTX), Ile-APP-induced apoptosis was totally blocked without decreasing the expression level of Ile-APP (Figure 4B). We next examined the effect of $G_o\alpha$G204A, an interfering mutant of $G_o\alpha$. As shown in Figure 4C, co-transfection of $G_o\alpha$G204A cDNA totally precluded the Ile-APP-expressing cells from apoptosis. In contrast, co-transfection of $G_{i2}\alpha$G204A cDNA had no effect on Ile-APP apoptosis under the same condition. Between these two co-transfections, the levels of Ile-APP expression were similar (data not shown). These results strongly indicated that the activity of G_o, not G_i, was involved in the action of Ile-APP.

We also tested the effect of Ile-APPΔ20, the Ile-APP mutant lacking cytoplasmic H657-K676. Expression of Ile-APPΔ20 in COS-NK1 cells failed to induce apoptosis, as assessed by both apoptotic changes of nuclei (Figure 4D) and nucleosomal DNA fragmentation (Figure 2C). The expression level and the cellular distribution of Ile-APPΔ20 did not differ from those of Ile-APP (Figure 1). Because H657-K676 is the demonstrated G_o-coupling domain of APP_{695} (Nishimoto *et al.*, 1993; Okamoto *et al.*, 1995), these data indicate the essential role of this cytoplasmic domain and the involvement of relevant G_o activation. Taking all these data together, Ile-APP should execute apoptosis through G_o.

In this study, it seemed unclear whether apoptosis, the shared phenotype of FAD-APPs, reflects the pathophysiology of FAD, since COS cells originated in the kidney. One possibility is to use neuronal cells, which are however disadvantageous in transfecting and expressing exogenous genes, although such a study is now in progress in our laboratory. In this study, we tried a different approach to substantiating the relationship between apoptosis by FAD-APP in COS-NK1 cells and the pathogenesis of FAD. The concept that AD is a multi-systemic disease (see below) allows this possible relationship. For this purpose, we examined the phenotypic linkage of FAD-APP-induced apoptosis in COS-NK1 cells to the FAD trait by carefully titrating the apoptosis-causing ability of FAD-APPs among all 19 possible V642 mutants. cDNA encoding each of APP_{695}, three FAD-APPs and all other 16 mutants was transfected into COS-NK1 cells, which resulted in similar expression and cellular distribution (not shown). As shown,

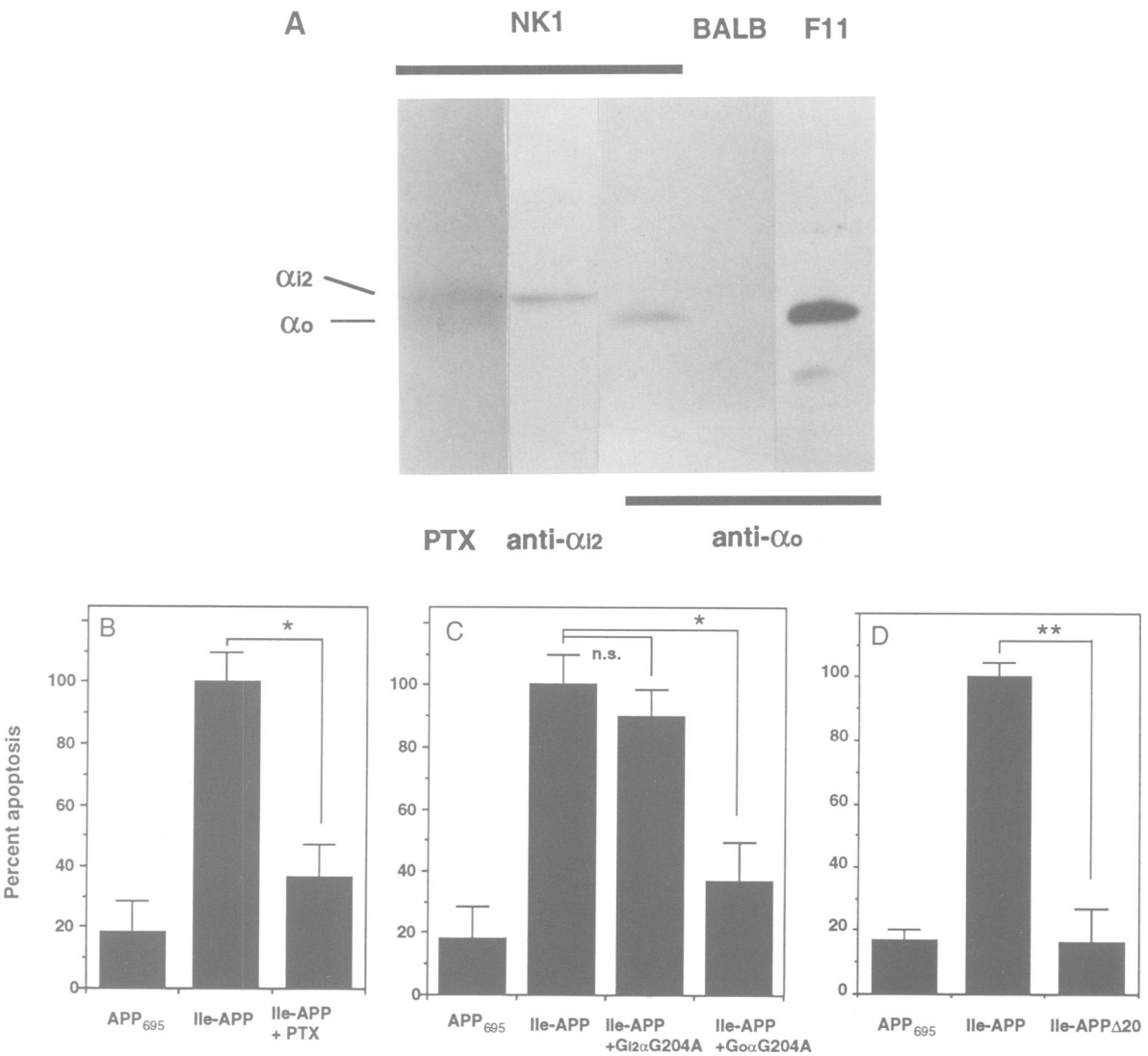

Fig. 4. Involvement of G_o in FAD-APP-induced apoptosis. (**A**) PTX-catalyzed ADP-ribosylation of COS-NK1 cells and immunoblot analysis of COS-NK1, BALB/c 3T3 and F11 cells are indicated. In the lane marked PTX, COS-NK1 cell membranes (100 μg) were ADP-ribosylated by PTX and applied to SDS–PAGE. In the four left lanes, cell membranes (100 μg) were analyzed with immunoblotting. Anti-α_{i2} and anti-α_o antibodies were described previously (Okamoto *et al.*, 1991). Samples were treated with *N*-ethylmaleimide (Evans *et al.*, 1986) and were loaded on modified Laemmli gels (Toutant *et al.*, 1987). F11 cells are hybridomas of a primary rat DRG neuron and a mouse neuroblastoma N18TG2 (Platika *et al.*, 1985). (**B**) PTX inhibits Ile-APP-induced apoptosis. COS-NK1 cells were transfected with 0.5 μg Ile-APP cDNA; at 24 h after transfection, culture media were changed to DME with 5 ng/ml PTX and 1% CS, and cells were cultured for another 24 h. The specific incidence of apoptosis by Ile-APP [(*b*/*a*)–*c* in Figure 2D] was measured. Apoptotic activity is indicated as a percentage of Ile-APP-induced apoptosis, which was 40.1, 40.1 and 42.8% in B, C and D, respectively. All values were means (± SE) of three independent sets of transfection. In each experiment, APP_{695} and Ile-APP cDNA were independently transfected. In these figures, the background incidence was similar to that in Figure 2D. (**C**) Ile-APP-induced apoptosis is inhibited by dominant-negative $G_o\alpha$, not by dominant-negative $G_{i2}\alpha$. After transfecting Ile-APP and $G_o\alpha$G204A cDNAs for 48 h, the specific incidence of apoptosis by Ile-APP expression cells was measured. Cells were also transfected with 0.5 μg APP_{695} cDNA or with Ile-APP and $G_{i2}\alpha$G204A cDNAs. (**D**) Ile-APPΔ20 totally loses the ability to induce apoptosis. COS-NK1 cells were transfected with 0.5 μg APP_{695}, Ile-APP or Ile-APPΔ20 cDNA. At 48 h after transfection, the incidence of apoptosis was assessed. $^*P < 0.05$; $^{**}P < 0.01$; n.s., not significant

the three FAD-APPs yielded the highest incidence of apoptosis among all other mutants, with wild-type APP_{695} the lowest (Figure 5). This experiment was independently repeated three times; each time, 20 individual cDNAs were transfected simultaneously. Notably, each experiment showed virtually the same order of apoptosis induction among APP mutants. Therefore, apoptosis by APP mutants was phenotypically linked to the FAD trait in our system, suggesting that apoptosis by FAD-APPs reflects a key pathological process of FAD.

Discussion

We have herein shown that three FAD-APPs, V642I, V642F and V642G, all cause COS-NK1 cells to undergo apoptosis. This study thus defines apoptosis to be a novel phenotype shared by the three FAD-APPs, which potentially explains the mechanism underlying FAD. It is also shown here that the cytoplasmic domain H657-K676 is critical for FAD-APP-induced apoptosis. Although the significance of apoptosis in AD has not been generally established, apoptosis is thought to be the most likely

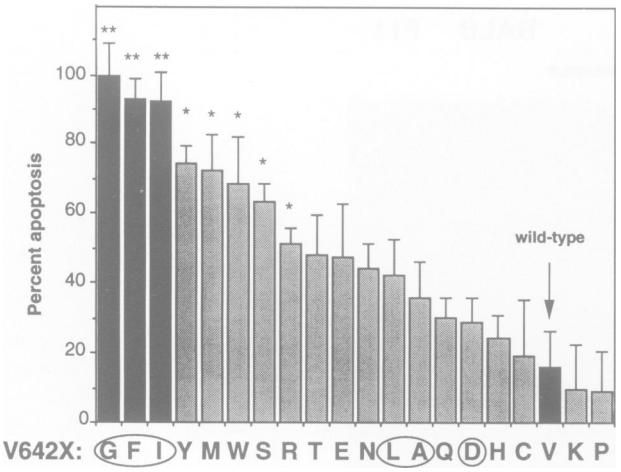

Fig. 5. Apoptosis by APP_{695} carrying a V642 substitution to each of all 19 residues. This figure shows incidence of apoptosis induced by V642X mutants of APP_{695} in COS-NK1 cells. COS-NK1 cells were transfected with each APP mutant cDNA, and the specific incidence of apoptosis was measured and indicated as a percentage of Gly-APP-induced apoptosis, which was 43.4%. Data indicate means (± SE) of three independent sets of simultaneous transfection. The residues that a single base mutation can make from GTC, the V642 codon of human APP_{695}, are encircled. $*P < 0.05$; $**P < 0.01$.

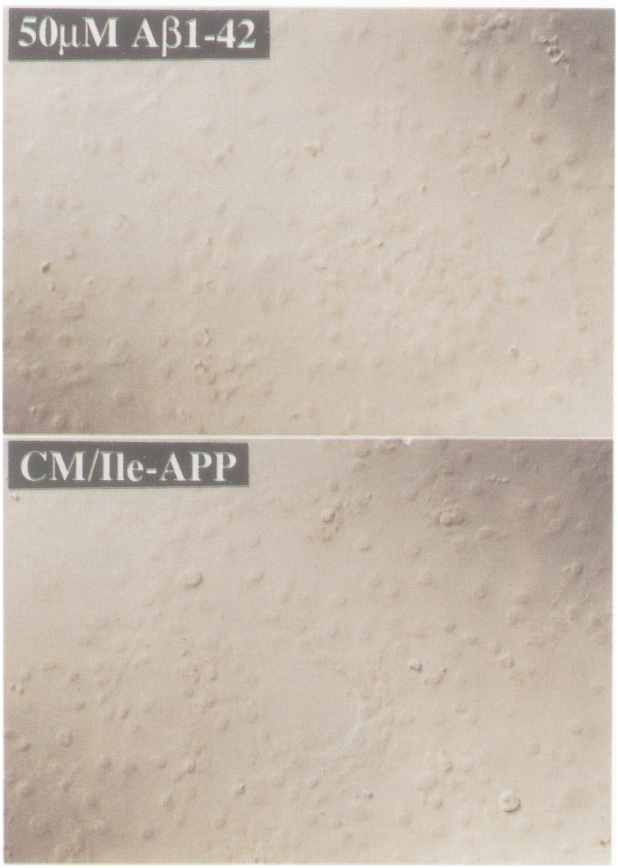

Fig. 6. Aβ1-42 or CM/COS-Ile-APP fails to induce apoptosis in COS-NK1 cells. Effects of 50 μM synthetic Aβ1-42 and CM/COS-Ile-APP were examined on nucleosomal DNA fragmentation in COS-NK1 cells. In the upper panel, COS-NK1 cells were cultured in the presence of 50 μM Aβ1-42 for 48 h, and DNA fragmentation was assessed with TUNEL. In the lower panel, COS-NK1 cells were cultured with CM/COS-Ile-APP for 48 h. CM/COS-Ile-APP represents the conditioned media obtained from COS-NK1 cells transfected with Ile-APP cDNA for 48 h, as in the legend of Figure 1.

candidate for the pathogenesis of this disease (Bredesen, 1994). Recently, Lassmann *et al.* (1995) evaluated cell death in AD brains using TUNEL, and concluded that ~30 times more cells showed DNA fragmentation in AD as compared with age-matched controls. The present study also shows that normal APP_{695} has little effect on apoptosis. This phenotypic dominance of FAD-APPs over normal APP fits well with the dominant inheritance of the FAD trait, suggesting a close relationship between this cytotoxic effect of FAD-APPs and the AD phenotype. In further support, the experiment with all possible V642 mutants revealed that apoptosis by APP mutants is phenotypically linked to the FAD trait in the present system. It should also be underscored that, except for I/F/G, A/D/L are all possible amino acids that a single base mutation can create from GTC, the V642 codon of human APP_{695}. The present data, indicating that none of the A/D/L changes yielded significant increase in apoptosis, are extremely consistent with the genetic results that I/F/G are all mutations that have been found in FAD. Taken together, apoptosis induced by FAD-APP in this system should reflect a key pathological process of FAD.

Evidence has accumulated indicating that AD is not merely a neuronal disease but a systemic disorder, as biochemical changes which mirror those in the brain have been detected in non-neuronal tissues including fibroblasts, lymphocytes and platelets (Peterson and Goldman, 1986; Huynh *et al.*, 1989; Blass *et al.*, 1991; Gibson and Toral-Barza, 1992; Molchan *et al.*, 1993; Ito *et al.*, 1994). Conversely, not all neuronal tissues are susceptible to Alzheimer disorders. Cerebellar neurons, for instance, are substantially spared from degeneration in this disease, despite diffuse Aβ deposition. Therefore, the tissue specificity of AD lesions does not fit into a classification focusing only on neurons and non-neurons. These facts suggest the presence of an as yet unidentified molecular basis which would produce such characteristic tissue specificity, and would also provide scientific grounds for the study of FAD-APP-induced cytotoxicity using non-neuronal cells. In addition, COS cells have an obvious advantage over neuronal cells with regard to growth velocity, transfection efficiency, and the high-level expression of exogenous genes. The present FAD-APP expression system using COS-NK1 cells thus deserves rigorous investigation as a model to analyze the mechanism for FAD-APP-induced cytotoxicity linked to FAD and to understand the basis for the tissue specificity of AD.

It is unlikely that humoral factors secreted from FAD-APP-expressing cells, including soluble APP, mediate apoptosis by FAD-APP, because (i) apoptosis only occurred in the same cell that expressed FAD-APP and (ii) the conditioned media of Ile-APP-transfected NK1 cells (CM/COS-Ile-APP) which were undergoing apoptosis caused virtually no apoptosis in untransfected NK1 cells (Figure 6). In addition to these different lines of evidence, we find it very unlikely that secreted Aβ1-40 mediates this response, because its secretion decreases from FAD-APP-expressing cells as compared with that from APP-expressing cells (Cai *et al.*, 1993; Suzuki *et al.*, 1994; Tamaoka *et al.*, 1994). Furthermore, 50 μM synthetic Aβ1-40 had no effect on nucleosomal DNA fragmentation

or on other apoptotic events in our system (data not shown).

We next focused on Aβ1-42, a longer version of Aβ. It should be stressed that secretion of this Aβ species increases from FAD-APP-expressing cells (Suzuki *et al.*, 1994) and that Aβ1-42 is the major (Tamaoka *et al.*, 1994) and the earliest (Iwatsubo *et al.*, 1994) constituent of senile plaques in AD. However, no significant DNA fragmentation was induced in COS-NK1 cells by 50 μM synthetic Aβ1-42 (Figure 6). This concentration was as high as near saturation of this peptide. Failure of apoptosis induction was also the case with CM/COS-Ile-APP supplemented with 50 μM synthetic Aβ1-42 (data not shown). Secondly, COS cells transfected with each of three FAD-APP cDNAs exhibited no augmentation in the net secretion of Aβ1-42 as compared with COS cells transfected with normal APP (Tamaoka *et al.*, 1994). In addition, the concentration of Aβ1-42 in the conditioned media of FAD-APP-transfected COS cells has been reported to be at picomolar levels (Tamaoka *et al.*, 1994). Thus, the failure of apoptosis by 50 μM Aβ1-42 with or without CM/COS-Ile-APP clearly indicates that secreted Aβ1-42 cannot mediate the apoptosis by FAD-APPs.

To exclude Aβ1-42 mediation definitely, we tested Ile-APPΔ41/42, a mutant Ile-APP which lacks the 41st and 42nd residues of the Aβ domain and hence encodes only Aβ1-40 but not Aβ1-42. This construct was expressed in COS-NK1 cells to a level comparable with that of Ile-APP (data not shown). Expression of Ile-APPΔ41/42 caused COS-NK1 cells to undergo apoptosis to a degree comparable with that induced by Ile-APP [84.5 ± 3.1% (mean ± SE, $n = 3$) of Ile-APP-induced specific apoptosis incidence]. Thus, the intermediary role of Aβ1-42 was very unlikely, suggesting an Aβ-independent mechanism whereby FAD-APPs induce cytotoxicity. This is however not surprising, as intracellular induction of an APP cytoplasmic tail causes cytotoxicity without increasing Aβ secretion (Hayashi *et al.*, 1992; Yoshikawa *et al.*, 1992).

Although the involvement of Aβ was less likely as far as FAD-APP-induced apoptosis in our system was concerned, this may not deny the significance of Aβ in the pathophysiology of AD. Aβ could be related to a number of other pathological processes and even to neuronal loss by its own mechanism. An important point is that there is a cellular mechanism whereby FAD-APP can cause cell death without mediation of secreted Aβ. This study does not exclude the possibility that Aβ1-42 cleavage, but not its secretion, may be involved in the mechanism of FAD-APP to trigger apoptosis. The oncogenic conversion of EGF receptor to v-erbB suggests that a receptor signal can be turned on by losing an extracellular regulatory portion. Given the fact that normal APP_{695} encodes a potential receptor (Okamoto *et al.*, 1995), it is conceivable that the augmented cleavage of Aβ1-42 from FAD-APP may turn on the death signal encoded by its cytoplasmic H657-K676 domain. Alternatively, FAD-APPs may turn on their cytotoxic effect through the mechanism totally independently of Aβ cleavage.

Of major interest are the findings indicating that heteromeric G proteins mediate FAD-APP-induced apoptosis. The evidence strongly suggests that the G protein is G_o. The PTX sensitivity indicated the involvement of G_i or G_o in FAD-APP-induced apoptosis, as PTX is a specific inhibitor of both G proteins. The experiments with $G_o\alpha$G204A or $G_{i2}\alpha$G204A clarified the selective role of G_o in apoptosis by FAD-APP. It has been established that these Gα mutant constructs act as dominant-negative mutants of the cognate Gα by sustaining an inactive GDP-bound conformation and thereby mask receptors from endogenous Gα (Hermouet *et al.*, 1991; Slepak *et al.*, 1993). Thus, the results indicated that the functional 'knockout' of $G_o\alpha$, not $G_i\alpha$, resulted in the abolition of apoptosis by Ile-APP. Furthermore, the failure of apoptosis by Ile-APPΔ20 provided an additional independent line of evidence for the involvement of G_o. Similar expression of Ile-APPΔ20 cDNA in the same system failed to induce apoptosis. Ile-APPΔ20 is the mutant Ile-APP specifically lacking the cytoplasmic H657-K676. Hence, the result indicates that this region plays a critical role in apoptosis by Ile-APP and that the target of this region is the mediator of FAD-APP apoptosis. It has been shown that: (i) the H657-K676 peptide is a G_o-specific activator; (ii) without this region, APP_{695} fails to bind G_o; (iii) recombinant APP_{695} couples to G_o but not G_i in vesicles and (iv) anti-H657-K676 monoclonal antibody blocks the coupling of APP_{695} to G_o (Nishimoto *et al.*, 1993; Okamoto *et al.*, 1995). Therefore, the known target of H657-K676 is only G_o and not G_i, which provides strong evidence that the PTX-sensitive G protein involved in Ile-APP-induced apoptosis is G_o. Taking all data together, G_o is the most likely mediator involved in the action of Ile-APP in the present system.

APP_{695} can interact directly with and activate G_o through H657-K676 (Okamoto *et al.*, 1995); the present study indicates that Ile-APP without H657-K676 loses the ability to induce apoptosis. It is thus highly likely that FAD-APPs turn on the apoptosis induction pathway by directly activating G_o. In fact, we have demonstrated that three FAD-APPs behave like constitutively activated G_o-coupled receptors in reconstituted vesicles (unpublished observation). G_o belongs to the heteromeric G protein family, which mediates signals of cell surface receptors to intracellular effectors. Although the action of G_o has not been well defined, accumulated evidence indicates a critical role of G_o in normal neuronal function and development (Hescheler *et al.*, 1987; Ito *et al.*, 1988; Goh and Pennefather, 1989; Granneman and Kapatos, 1990; Guillén *et al.*, 1990; Strittmatter *et al.*, 1990, 1994; Igarashi *et al.*, 1993). G_o is a major membrane protein in the brain (Huff *et al.*, 1985) and is concentrated in the gray matter and hippocampus, which corresponds well to the brain areas severely afflicted by AD. At first, G_o was thought to be limited to neurons and neuroendocrine cells, but was later reported in various tissues and cells (Toutant *et al.*, 1987; Olate *et al.*, 1989; Spicher *et al.*, 1991; Sebok *et al.*, 1993; Baffy *et al.*, 1994; Mulheron *et al.*, 1994). Although the mechanism of G protein-linked apoptosis needs further investigation, this study delineates a novel intracellular messenger system for cell death by FAD-APPs.

The intermediary role of G proteins in the action of FAD-APP opens up a new idea: various insults causing activation of the G protein could induce pathophysiology at least partly similar to that induced by FAD-APPs. This is also the case with the downstream pathway of G proteins; those which bypass G proteins and activate the

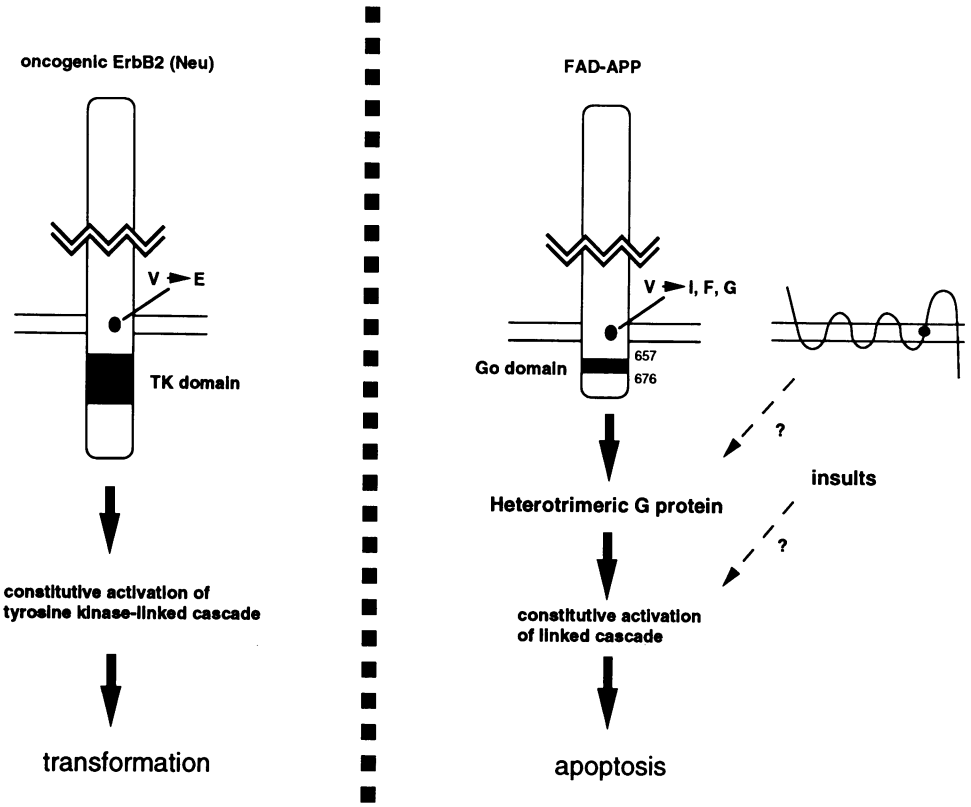

Fig. 7. The Neu transformation system and the FAD-APP apoptosis system. Right: this study shows that FAD-APP induces apoptosis through G-protein activation. Thus, it is reasonable to assume that any other G-coupled receptor mutants with constitutive activity could induce biological abnormalities similar to those induced by FAD-APP. In fact, a protein with seven putative transmembrane domains has been identified as being responsible for FAD linked to chromosome 14 (Sherrington *et al.*, 1995). This theory also allows for the possibility that the insults bypassing the G protein and activating its downstream pathway could cause cellular malfunction similar to that induced by FAD-APP. Left: c-ErbB2 is a normal receptor tyrosine kinase and is converted to oncogenic Neu by transmembrane V664E. Neu has autoactive kinase and causes transformation, whereas c-ErbB2 has no transforming activity. In the FAD-APP system, activation of the downstream machinery by FAD mutations causes apoptotic cell death, whereas normal APP has no such activity. In both cases, point mutations of receptors induce dominant abnormality in their effector systems and cause cellular malfunctions that are probably critical processes of the diseases.

downstream targets could mimic abnormalities induced by FAD-APPs. This novel theory allows for the possibility that various causes may induce similar or the same type of AD and may well explain the conclusion of genetic analysis that AD is a heterogeneous disease caused by abnormalities of various genes. Recently, the chromosome 14 gene responsible for another type of FAD has been identified and shown to encode a membrane integral protein with seven putative transmembrane domains (Sherrington *et al.*, 1995). As such structured proteins are most likely G protein-coupled receptors, this discovery might provide strong support for the concept that abnormality in G protein-linked pathways is a common promoter of AD, although the real function of this protein remains unknown.

This study also highlights the similar mechanistic frameworks in the Neu-induced transformation system and the FAD-APP-induced apoptosis system (Figure 7). In the former system, activation of the downstream machinery by the Neu mutation leads to transformation (Bargmann *et al.*, 1986). In the FAD-APP system, activation of the downstream machinery by the FAD mutations likely causes apoptosis. In both cases, point mutations in the transmembrane domains of cell surface molecules induce a dominant abnormality in their effector systems. These cellular malfunctions (transformation and apoptosis) are probably essential processes in the mechanism of diseases such as cancer and AD. As studies of tyrosine kinases have provided a growing body of information useful in cancer research, further studies of FAD-APP-induced apoptosis are expected to contribute significantly to analyzing and developing therapies for this disease.

Finally, the question must be addressed of why the apoptotic effect of FAD-APP is considerably rapid, when it takes many years for FAD to develop. One possibility is that expression of the cell death apparatus necessary for this effect of FAD-APP is age-dependent. The mechanism underlying this effect should thus be further delineated. Alternatively, in asymptomatic kindreds, the cell death effect of FAD-APP may be antagonized by a certain defense mechanism of the body, which deteriorates after several decades of life. In this regard, it is quite interesting that many cytokines and serum factors have been reported to antagonize apoptosis in a cell death-specific manner.

Materials and methods

Materials

Human *bcl-2* cDNA under the control of the SV40 promoter, provided by Drs S.J.Korsmeyer (Washington University, MO) and J.Yuan

(Massachusetts General Hospital, MA) and *lacZ* gene under the control of the β-actin promoter, were from Dr J.Yuan (Miura *et al.*, 1993). $G_o\alpha$G204A cDNA was provided by Dr S.M.Strittmatter (Strittmatter *et al.*, 1994). Aβ1-40 and Aβ1-42 were purchased from Sigma and Backem, respectively.

Construction of mutants

For construction of APP mutants, the *Sac*I–*Bam*HI fragment of mouse APP_{695} cDNA (Nishimoto *et al.*, 1993) was initially subcloned in M13mp18. Oligonucleotide-directed mutagenesis was conducted by the Kunkel method. The *Sac*I–*Xba*I fragment of each APP mutant cDNA was inserted into pVL1393-APP (Nishimoto *et al.*, 1993). We used ACCGTGATTATCATCACCC for V642I, ACCGTGATTTTCATCACCC for V642F, CCGTGATTGGCATCACCCT for V642G, CCGTGATTCGCATCACCCT for V642R, ACCGTGATTCTCATCACCC for V642L, CCGTGATTGACATCACCCT for V642D, CCGTGATTGCCATCACCCT for V642A, CCGTGATTTACATCACCCT for V642Y, CCGTGATTTGCATCACCCT for V642C, CCGTGATTTCCATCACCCT for V642S, CCGTGATTAACATCACCCT for V642N, CCGTGATTACCATCACCCT for V642T, CGTGATTATGATCACCCTG for V642M, CCGTGATTCACATCACCCT for V642H, CCGTGATTCCCATCACCCT for V642P, CGTGATTGAGATCACCCTG for V642E, CGTGATTTGGATCACCCTG for V642W, ACCGTGATTAAGATCACCC for V642K, ACCGTGATTCAGATCACCC for V642Q and GATGATAATCACGGTGACAACGCCGCC-CAC for Ile-APPΔ41/42. All mutations were verified by DNA sequencing. The *Bam*HI fragment of each APP mutant was subcloned into pcDNA1. Ile-APPΔ20 was constructed using the following primers: AAACAGTACACATCCATCATGCAGCAG (Internal primer IP1) and ATATCCGTTCTGCTGCATGATGGATGT (IP2) and AACGACGCTCTCATGCCT (External primer EP1) and AATGGGGAAGCTGTCTTCCAT (EP2). After amplification of two fragments of Ile-APP cDNA by PCR using two combinations of the primers (EP1/IP2 and EP2/IP1), those fragments were mixed and amplified by PCR using the two external primers to generate a fragment lacking H657-K676. This fragment was subcloned into pVL-APP (Nishimoto *et al.*, 1993), utilizing *Sac*I and *Xba*I restriction sites. The sequence was verified to lack H657-K676 and not to contain the unwanted mutation in the region which was through PCR. The entire Ile-APPΔ20 fragment (~2 kb) was recovered with *Bam*HI digestion and subcloned into pcDNA1. Some of the APP constructs were also subcloned into pECE, which yielded similar results.

Cell clones

We screened COS cell clones that significantly express $G_o\alpha$ immunoreactivity, and a clone was selected (Figure 4A). It was named COS-NK1, which was originally a COS-7 clone provided by K.Bloch (Massachusetts General Hospital, MA), grown in Dulbecco's modified Eagle's medium (DME) supplemented with 10% CS and streptomycin/penicillin, and used in this study. No significant apoptosis was induced by FAD-APPs in usual COS-7 cells obtained from ATCC. For transient transfection, NK1 cells were seeded at 4×10^4/well in a 24-well plate or at 10^6/dish in a 100-mm dish and cultured for 24 h in DME plus 10% CS and penicillin/streptomycin. Cells were transfected with cDNA and LipofectAMINE (Gibco) (cDNA and LipofectAMINE, 0.5 μg and 1 μl in a 24-well plate for ELISA, TUNEL and immunohistochemical assay; 10 μg and 20 μl in a 100-mm dish for immunoblotting and DNA laddering) in DME. This protocol yielded similar expression of cDNAs between these two settings. Media were changed to DME plus 1% CS after 24-h serum-free culture. After another 24-h culture, cells were fixed or lysed. For stable expression of *bcl-2*, COS-NK1 cells were transfected by the calcium phosphate method using 10 μg *bcl-2* cDNA in pBabe/Puro. Cells were selected with 3 μg/ml puromycin. After 2–3 weeks, a clone was chosen and amplified for future studies.

Fragmented DNA associated with histone was detected using an ELISA kit (Boehringer Mannheim) according to the manufacturer's instructions. Cells were seeded onto 24-well plates 24 h before transfection. After transfection, cell lysates were centrifuged for 10 min at 15 000 r.p.m. and the supernatants loaded on wells precoated with anti-histone antibody. After washing, labeled anti-DNA antibody was loaded on those wells. ABTS was added and OD_{405}/OD_{492} measured by a microplate reader.

Ladder assays

For the ladder assay, DNA was extracted from cells treated with lysis buffer (100 mM Tris–HCl, pH 8.5, 5 mM EDTA, 0.2% SDS, 200 mM NaCl, 100 μg/ml Proteinase K). The cell lysate was incubated at 37°C for 4 h with agitation, and subjected to isopropanol precipitation, two phenol/chloroform extractions and ethanol precipitation. The extracted DNA was finally resolved in TE buffer (10 mM Tris–HCl, pH 8.0 and 1 mM EDTA), to which 10 μg/ml RNase was added. The nucleosomal-size ladder of DNA was visualized in an agarose gel, as described (Rösl, 1992). Briefly, the sample (1 μg DNA) was incubated with 5 U Klenow polymerase and 0.5 μCi [^{32}P]dCTP in 10 mM Tris–HCl, pH 7.5 and 5 mM $MgCl_2$ for 10 min. The reaction was terminated by addition of 10 mM EDTA and incubation for 10 min at 75°C. The unincorporated nucleotides were removed by three consecutive precipitation cycles of 2.5 M ammonium acetate/isopropanol, and the labeled DNA was resuspended in the TE buffer. The sample (0.25 μg DNA) was subjected to 1.8% agarose gel electrophoresis and autoradiography.

Immunohistochemical analysis and TUNEL

Immunohistochemical analysis and nuclear staining were performed as described by Miura *et al.* (1993). The sample was fixed in methanol/acetone at –20°C for 5 min, dried, incubated with PBS plus 1% BSA and 5% CS for 1 h, incubated with 22C11 (0.5 μg/ml) for 2 h, washed with PBS, incubated with Texas Red-labeled anti-mouse IgG (Jackson ImmunoResearch, 1/100) for 45 min, washed with PBS and incubated with 5 μM acridine orange for 5–10 min. Samples were examined with a fluorescence microscope. For the X-Gal staining, cells were washed with PBS, fixed with 2.5% glutaraldehyde, 2 mM $MgCl_2$, 2 mM EGTA in PBS for 10 min and stained with X-Gal buffer with 0.1% Triton X-100 for 1 h.

TUNEL was performed with a kit distributed by Oncor. COS-NK1 cells (4×10^4/well) were seeded onto a slide glass set inside a 24-well plate in the presence of complete media. After similarly performed transfection and incubation, the slide glass was subjected to procedures for TUNEL, according to the manufacturer's instructions.

The profiles of the time-course of apoptosis detected by the assays used in this study (DNA laddering, ELISA, TUNEL and nuclear morphology) were each different, depending on the aspect of apoptosis focused on in each assay. To begin detecting apoptotic abnormality at a significant level, the DNA laddering assay took 12 h after transfection of FAD-APP cDNAs, the ELISA and TUNEL assays needed 24 h, and the nuclear morphology assay required 36 h. The optimal time points were 24, 24–48 and 48 h, respectively, based on where we set the period for each assay. However, the expression timing of transfected cDNA was not synchronized, and APP mutants were randomly expressed in cells during 2–3 days post-transfection. It is therefore underscored that the time-dependency, which was different among these assays, did not reflect the sequential events of apoptosis occurring in an individual cell.

All results presented in this study were repeated at least three times, and most more than five times, with independent sets of transfection, each of which yielded similar results. Statistical significance was determined with Student's *t* test.

Acknowledgements

We thank M.C.Fishman, T.B.Kinane and K.Yonezawa for critical reading of this manuscript and indispensable advice; M.Miura and J.Yuan for *lacZ* and *bcl-2* genes and technical supervision; S.J.Korsmeyer for *bcl-2* gene; S.M.Strittmatter for $G_o\alpha$G204A cDNA; Y.Tamai, E.Ogata and S.Seino for indispensable support; and D.Wylie and U.Giambarella for expert technical assistance. This work was supported in part by Bristol-Myers Squibb.

References

Baffy,G., Yang,L., Raj,S., Manning,D.R. and Williamson,J.R. (1994) G protein coupling to the thrombin receptor in Chinese hamster lung fibroblasts. *J. Biol. Chem.*, **269**, 8483–8487.

Bargmann,C.I., Hung,M.C. and Weinberg,R.A. (1986) Multiple independent activations of the neu oncogene by a point mutation altering the transmembrane domain of p185. *Cell*, **45**, 649–657.

Blass,J.P., Baker,A.C., Ko,L.-W., Sheu,R.K.-F. and Black,R.S. (1991) Expression of 'Alzheimer antigens' in cultured skin fibroblasts. *Arch. Neurol.*, **48**, 709–717.

Bredesen,D.E. (1994) Neuronal apoptosis: genetic and biochemical modulation. In Tomei,L.D. and Frederick,F.O. (eds), *Apoptosis II.* Cold Spring Harbor Laboratory Press, Cold Spring Harbor, NY, pp. 397–421.

Cai,X.-D., Golde,T.E. and Younkin,S.G. (1993) Release of excess amyloid β protein from a mutant amyloid β protein precursor. *Science*, **259**, 514–516.

Doherty,P., Ashton,S.V., Moore,S.E. and Walsh,F.S. (1991) Morphoregulatory activities of NCAM and N-cadherin can be accounted for by G protein-dependent activation of L- and N-type neuronal Ca^{2+} channels. *Cell*, **67**, 21–33.

Evans,T., Brown,M.L., Fraser,E.D. and Northup,J.K. (1986) Purification of the major GTP-binding proteins from human placental membranes. *J. Biol. Chem.*, **261**, 7052–7059.

Games,D. *et al.* (1995) Alzheimer-type neuropathology in transgenic mice overexpressing V717F β-amyloid precursor protein. *Nature*, **373**, 523–527.

Gavrieli,Y., Sherman,Y. and Ben-Sasson,S.A. (1992) Identification of programmed cell death *in situ* via specific labeling of nuclear DNA fragmentation. *J. Cell Biol.*, **119**, 493–501.

Gibson,G.E. and Toral-Barza,L. (1992) Cytosolic free calcium in lymphoblasts from young, aged and Alzheimer subjects. *Mech. Ageing Dev.*, **63**, 1–9.

Goate,A. *et al.* (1991) Segregation of a missense mutation in the amyloid precursor protein gene with familial Alzheimer's disease. *Nature*, **349**, 704–706.

Goh,J.W. and Pennefather,P.S. (1989) A pertussis toxin-sensitive G protein in hippocampal long-term potentiation. *Science*, **244**, 980–983.

Granneman,J.G. and Kapatos,G. (1990) Developmental expression of G_o in neuronal cultures from rat mesencephalon and hypothalamus. *J. Neurochem.*, **54**, 1995–2001.

Guillén,A., Jallon,J.-M., Fehrentz,J.-A., Pantaloni,C., Bockaert,J. and Homburger,V. (1990) A G_o-like protein in *Drosophila melanogaster* and its expression in memory mutants. *EMBO J.*, **9**, 1449–1455.

Hardy,J. (1992) Framing β-amyloid. *Nature Genet.*, **1**, 233–234.

Hayashi,Y., Kashiwagi,K. and Yoshikawa,K. (1992) Protease inhibitors generate cytotoxic fragments from Alzheimer amyloid protein precursor in cDNA-transfected glioma cells. *Biochem. Biophys. Res. Commun.*, **187**, 1249–1255.

Hermouet,S., Merendino,J.J.,Jr, Gutkind,J.S. and Siegel,A.M. (1991) Activating and inactivating mutations of the α subunit of G_{i2} protein have opposite effects on proliferation of NIH3T3 cells. *Proc. Natl Acad. Sci. USA*, **88**, 10455–10459.

Hescheler,J., Rosenthal,W., Trautwein,W. and Schultz,G. (1987) The GTP-binding protein G_o, regulates neuronal calcium channels. *Nature*, **325**, 445–447.

Huff,R.M., Axton,J.M. and Neer,E. (1985) Physical and immunological characterization of a guanine nucleotide-binding protein purified from bovine cerebral cortex. *J. Biol. Chem.*, **260**, 10864–10871.

Huynh,V.T., Cole,G., Katzman,R., Huang,K.-P. and Saitoh,T. (1989) Reduced protein kinase C immunoreactivity and altered protein phosphorylation in Alzheimer's disease fibroblasts. *Arch. Neurol.*, **46**, 1195–1199.

Igarashi,M., Strittmatter,S.M., Vartanian,T. and Fishman,M.C. (1993) Mediation by G proteins of signals that cause collapse of growth cones. *Science*, **259**, 77–79.

Ito,E., Oka,K., Etcheberrigaray,R., Nelson,T.J., McPhie,D.L., Tofel-Grehl,B., Gibson,G.E. and Alkon,D.L. (1994) Internal Ca^{2+} mobilization is altered in fibroblasts from patients with Alzheimer's disease. *Proc. Natl Acad. Sci. USA*, **91**, 534–538.

Ito,I., Okada,D. and Sugiyama,H. (1988) Pertussis toxin suppresses long-term potentiation of hippocampal mossy fiber synapses. *Neurosci. Lett.*, **90**, 181–185.

Iwatsubo,T., Odaka,A., Suzuki,N., Mizusawa,H., Nukina,N. and Ihara,Y. (1994) Visualization of Aβ42(43) and Aβ40 in senile plaques with end-specific Aβ monoclonals: evidence that an initially deposited species is Aβ42(43). *Neuron*, **13**, 45–53.

Jacobson,M.D., Burne,J.F., King,M.P., Miyashita,T., Reed,J.C. and Raff,M.C. (1993) Bcl-2 blocks apoptosis in cells lacking mitochondrial DNA. *Nature*, **361**, 365–369.

Kang,J., Lemaire,H.-G., Unterback,A., Salbaum,J.M., Masters,C.L., Grezeschik,K.H., Multhaup,G., Beyreuther,K. and Müller-Hill,B. (1987) The precursor of Alzheimer disease amyloid A4 protein resembles a cell-surface receptor. *Nature*, **325**, 733–736.

Karlinsky,H. *et al.* (1992) Molecular and prospective phenotypic characterization of a pedigree with familial Alzheimer's disease and a missense mutation in codon 717 of the β-amyloid precursor protein gene. *Neurology*, **42**, 1445–1453.

Kerr,J.F.R. and Harmon,B.V. (1991) Definition and incidence of apoptosis: an historical perspective. In Tomei,L.D. and Cope,F.O. (eds), *Apoptosis, The Molecular Basis of Cell Death*. Cold Spring Harbor Laboratory Press, Cold Spring Harbor, NY, pp. 5–29.

Lassmann,H., Bancher,C., Breitschopf,H., Wegiel,J., Bobinski,M., Jellinger,K. and Wisniewski,H.M. (1995) Cell death in Alzheimer's disease evaluated by DNA fragmentation *in situ*. *Acta Neuropathol.*, **89**, 35–41.

Mattson,M.P., Cheng,B., Culwell,A.R., Esch,F.S., Liebergurg,I. and Rydel,R.E. (1993) β-Amyloid precursor protein metabolites and loss of neuronal Ca^{2+} homeostasis in Alzheimer's disease. *Trends Neurosci.*, **16**, 409–414.

Milward,E.A., Papadopoulos,R., Fuller,S.J., Moir,R.D., Small,D., Beyreuther,K. and Masters,C.L. (1992) The amyloid protein precursor of Alzheimer's disease is a mediator of the effects of nerve growth factor on neurite outgrowth. *Neuron*, **9**, 129–137.

Miura,M., Zhu,H., Rotello,R., Hartwieg,E.A. and Yuan,J. (1993) Induction of apoptosis in fibroblasts by IL-1β-converting enzyme, a mammalian homolog of the *C. elegans* cell death gene *ced-3*. *Cell*, **75**, 653–660.

Molchan,S.E., Manji,H., Chen,G., Dou,L., Little,J., Potter,W.Z. and Sunderland,T. (1993) Effects of chronic lithium treatment on platelet PKC isoenzymes in Alzheimer's and elderly control subjects. *Neurosci. Lett.*, **162**, 187–191.

Mönning,U., König,G., Banati,R.B., Mechlert,H., Czech,C., Gehrmann,J., Schreiter-Gasser,U., Masters,C.L. and Beyreuther,K. (1992) Alzheimer βA4-amyloid protein precursor in immunocompetent cells. *J. Biol. Chem.*, **267**, 23950–23956.

Mulheron,J.G., Casañas,S.J., Arthur,J.M., Garnovskaya,M.N., Gettys,T.W. and Raymond,J.R. (1994) Human $5\text{-}HT_{1A}$ receptor expressed in insect cells activates endogenous G_o-like G protein(s). *J. Biol. Chem.*, **269**, 12954–12962.

Müller,U., Cristina,N., Li,Z.-W., Wolfer,D.P., Lipp,H.-P., Rülicke,T., Brandner,S., Aguzzi,A. and Weissmann,C. (1994) Behavioral and anatomical deficits in mice homozygous for a modified β-amyloid precursor protein gene. *Cell*, **79**, 755–765.

Nishimoto,I., Okamoto,T., Matsuura,Y., Okamoto,T., Murayama,Y. and Ogata,E. (1993) Alzheimer amyloid protein precursor forms a complex with brain GTP binding protein G_o. *Nature*, **362**, 75–79.

Okamoto,T., Takeda,S., Murayama,Y., Ogata,E. and Nishimoto,I. (1995) Ligand-dependent G protein coupling function of amyloid transmembrane precursor. *J. Biol. Chem.*, **270**, 4205–4208.

Olate,J., Jorquera,H., Purcell,P., Codina,J., Birnbaumer,L. and Allende,J.E. (1989) Molecular cloning and sequence determination of a cDNA coding for the α-subunit of a G_o-type protein of *Xenopus laevis* oocytes. *FEBS Lett.*, **244**, 188–192.

Peterson,C. and Goldman,J.E. (1986) Alterations in calcium content and biochemical processes in cultured skin fibroblasts from aged and Alzheimer donors. *Proc. Natl Acad. Sci. USA*, **83**, 2758–2762.

Platika,D., Boulos,M.H., Baizer,L. and Fishman,M.C. (1985) Neuronal traits of clonal cell lines derived by fusion of dorsal root ganglia neurons with neuroblastoma cells. *Proc. Natl Acad. Sci. USA*, **82**, 3499–3503.

Rösl,F. (1992) A simple and rapid method for detection of apoptosis in human cells. *Nucleic Acids Res.*, **20**, 5243.

Sandbrink,R., Masters,C.L. and Beyreuther,K. (1994) βA4-amyloid protein precursor mRNA isoforms without exon 15 are ubiquitously expressed in rat tissues including brain, but not in neurons. *J. Biol. Chem.*, **269**, 1510–1517.

Schubert,W., Prior,R., Weidemann,A., Dircksen,H., Multhaup,G., Masters,C.L. and Beyreuther,K. (1991) Amyloid β protein precursor is a mitogen. *Brain Res.*, **563**, 184–194.

Schuch,U., Lohse,M.J. and Schachner,M. (1989) Neural cell adhesion molecules influence second messenger systems. *Neuron*, **3**, 13–20.

Sebok,K., Woodside,D., Al-Aoukaty,A., Ho,A.D., Gluck,S. and Maghazachi,A.A. (1993) IL-8 induces the locomotion of human IL-2-activated natural killer cells. Involvement of a guanine nucleotide binding (G_o) protein. *J. Immunol.*, **150**, 1524–1534.

Sherrington,R. *et al.* (1995) Cloning of a gene bearing missense mutations in early-onset familial Alzheimer's disease. *Nature*, **375**, 754–760.

Slepak,V.Z., Wilkie,T.M. and Simon,M.I. (1993) Mutational analysis of G protein α subunit $G_o\alpha$ expressed in *Escherichia coli*. *J. Biol. Chem.*, **268**, 1414–1423.

Small,D.H., Nurcombe,V., Reed,G., Clarris,H., Moir,R., Beyreuther,K. and Masters,C.L. (1994) A heparin-binding domain in the amyloid protein precursor of Alzheimer's disease is involved in the regulation of neurite outgrowth. *J. Neurosci.*, **14**, 2117–2127.

Spicher,K., Klinz,F.-J., Rudolph,U., Codina,J., Birnbaumer,L., Schultz,G. and Rosenthal,W. (1991) Identification of the G-protein α-subunit encoded by $\alpha_o 2$ cDNA as a 39 kDa pertussis toxin substrate. *Biochem. Biophys. Res. Commun.*, **175**, 473–478.

Strittmatter,S.M., Valenzuela,D., Kennedy,T.E., Neer,E.J. and Fishman,M.C. (1990) G_o is a major growth cone protein subject to regulation by GAP-43. *Nature*, **344**, 836–841.

Strittmatter,S.M., Fishman,M.C. and Zhu,X.-P. (1994) Activated mutants of the α subunit of G_o promote an increased number of neurites per cell. *J. Neurosci.*, **14**, 2327–2338.

Suzuki,N., Cheung,T.T., Cai,X.-D., Odaka,A., Otvos,L., Eckman,C., Golde,T.E. and Younkin,S.G. (1994) An increased percentage of long amyloid β protein secreted by familial amyloid β protein precursor (βAPP_{717}) mutants. *Science*, **264**, 1336–1340.

Tamaoka,A. *et al.* (1994) APP717 missense mutation affects the ratio of amyloid β protein species (Aβ1-42/43 and Aβ1-40) in familial Alzheimer's disease brain. *J. Biol. Chem.*, **269**, 32721–32724.

Toutant,M., Aunis,D., Bockaert,J., Homburger,V. and Rouot,B. (1987) Presence of three pertussis toxin substrates and $G_o\alpha$ immunoreactivity in both plasma and granule membranes of chromaffin cells. *FEBS Lett.*, **215**, 339–344.

Ueda,K., Cole,G., Sundsmo,M., Katzman,R. and Saitoh,T. (1989) Decreased adhesiveness of Alzheimer's disease fibroblasts: is amyloid β-protein precursor involved? *Ann. Neurol.*, **25**, 246–251.

Yoshikawa,K., Aizawa,T. and Hayashi,Y. (1992) Degeneration *in vitro* of post-mitotic neurons overexpressing the Alzheimer amyloid protein precursor. *Nature*, **359**, 64–67.

Zheng,H. *et al.* (1995) β-Amyloid precursor protein-deficient mice show reactive gliosis and decreased locomotor activity. *Cell*, **81**, 525–531.

Received on August 14, 1995; revised on October 2, 1995